Chapter 4

The fate of bacterial carbon in sediments: Modeling an in situ isotope tracer experiment

Dick van Oevelen, Jack J. Middelburg, Karline Soetaert and Leon Moodley. *Accepted by Limnology and Oceanography*

4.1 Introduction

Biogeochemical cycling in marine soft sediments is dominated by heterotrophic bacterial communities (Smith, 1973). Although being highly diverse in terms of species (Torsvik et al., 1996; Li et al., 1999) and metabolic strategies (Fenchel et al., 1998), total bacterial numbers are comparatively constant at around 10^9 bacteria ml^{-1} porewater (Schmidt et al., 1998). Irrespective of this constancy, specific growth rates vary by four orders of magnitude (Sander and Kalff, 1993). The importance of bacteria in early diagenetic processes and their potential as food source has generated ample interest in the processes affecting bacterial carbon in sediments, a topic that is basically approached from at least three directions: 1) bottom-up control, 2) biogeochemical approach and 3) top-down control.

The bottom-up approach has focussed on finding linear relationships between particulate organic matter and bacterial biomass or production. These relationships may be spurious for various reasons (Bird and Duarte, 1989; Flemming and Delafontaine, 2000), but when standardized to volumetric units, significant relationships explain 25 - 60 % of the observed variation in bacterial biomass (Schallenberg and Kalff, 1993) and production (Sander and Kalff, 1993), suggesting that substrate availability impacts bacterial dynamics.

Biogeochemists usually focus on hydrolysis rates of standardized substrates (Meyer-Reil, 1986; Sawyer and King, 1993; Arnosti and Holmer, 1999) or sediment dissolved organic matter (Alperin et al., 1994; Burdige et al., 1999), production of bacterial biomass (Dixon and Turley (2001) and references therein), respiration and growth efficiency (Jahnke and Craven, 1995; del Giorgio and Cole, 1998). Hence, the biogeochemical approach resolves rates of oxic, suboxic and anoxic mineralization pathways, but the fate of bacterial production is not explicitly studied.

In the top-down approach, bacterial carbon is assumed to be regulated by higher trophic levels of the benthic food web, a topic which has a long-standing interest dating back to the 1930's (MacGinitie, 1932; ZoBell, 1938). In a seminal review on bacterivory, Kemp (1990) asserted that bacteria do not form an important constituent of the macrobenthic diet and concluded that reports for meiobenthos (mostly nematodes) were conflicting. It was however noted that quantitative bacterivory data of meiobenthos and protozoans were either sparse or lacking. Methodological advances have been made such as the use of fluorescent stained sediment (Starink et al., 1994) and radioactively labeled substrates (Montagna, 1995). Using these methods, quantitative data on bacterivory by small-sized grazers have been gathered (Epstein et al., 1992; Sundback et al., 1996; Hamels et al., 2001b). In general, only 1 - 20 % of the bacterial production is grazed, although grazing intensity may fluctuate seasonally (Hondeveld et al., 1995; Epstein, 1997b; Hamels et al., 2001b). Grazing studies are generally focussed on the top cm of the sediment and are based on comparatively short time incubations (minutes to hours) in retrieved and/or slurried sediments, rendering translation to the field and longer periods cumbersome. In addition, bacterial production is measured by other methods than bacterivory and therefore do not form an integral part of the grazing studies.

Another top down agent that has received interest is viral infection (Maranger and Bird, 1996; Fischer et al., 2003; Hewson and Fuhrman, 2003), which potentially exerts control on bacteria through infection and subsequent cell lysis (Weinbauer, 2004). This mechanism may set upper limits on bacterial biomass or production, but leaves unexplained the subsequent fate of the bacterially derived carbon. Studies carried out in continental margin sediments show burial of recalcitrant bacterial cell wall remnants (Grutters et al., 2002). However, Novitsky (1986) reported rapid mineralization of dead microbial biomass in a tropical marine beach sediment.

It is clear that several regulating factors act upon sedimentary bacteria and a comprehensive understanding calls for the integration of bottom-up, biogeochemical and top-down approaches. Boudreau (1999) provided such an integration by developing spatial and temporal mass balance equations of bacterial carbon in sediments and used these in a theoretical investigation to explain the observed linear relationships between bacterial biomass and sediment particulate organic carbon (POC). The parameters of this linear relationship are non-linear composites of parameters describing exchange processes, bacterial growth efficiency and biological processes including growth, mortality and grazing.

We report the results of a ^{13}C-glucose labeling experiment and use these data in a tracer model to quantify the fate of sedimentary bacterial carbon. ^{13}C-glucose was injected in intertidal sediments and traced into bacterial specific polar-lipid-derived fatty acids (PLFAs), total organic carbon, meiobenthos, macrobenthos and respired carbon during a period of 4.5 months. The modeled processes were selected based on the comprehensive analysis by Boudreau (1999). The combined modeling – ^{13}C tracer study allowed us to quantify bacterial production, bacterial growth efficiency, mortality, resuspension and bacterial grazing by meiobenthos and macrobenthos.

4.2 Material and methods

4.2.1 Experimental approach

The Molenplaat intertidal flat was chosen as the study site since detailed physical and biological background data are available (Herman et al., 2001). The intertidal flat is located in the saline part (salinity 20-25) of the turbid, heterotrophic and nutrient-rich Scheldt estuary. The sampling site is located in the muddy center of the flat (51°26.25' N, 3°57.11' E), has a median grain size of 77 μm, organic carbon content of $\sim$ 0.5 wt % and exposure time of about 7 hours per tidal cycle.

Prior to labeling, two 0.25 m^{-2} metal frames (0.5x0.5x0.08 m) were inserted in the sediment. On 21 May 2003, the upper 10 cm was labeled in two hours with ^{13}C by injecting 0.4 ml glucose solution (23.5 mmol ^{13}C l^{-1}) into four hundred 6.25 cm^{-2} squares $plot^{-1}$, which resulted in a flux of 15.3 mmol ^{13}C m^{-2} per labeling day. Labeling was performed daily for 5 consecutive days to ensure sufficient label incorporation by bacteria, but labeling on day 2 had to be canceled due to bad weather. S

ampling frequency was high initially (day 0, 0.2, 2, 3, 4, 5, 6, 8, 12, 18) and lower thereafter (day 36, 71, 136). On each sampling day, one sampling core was taken per plot. Sampling positions within the plots were determined a priori by a randomization procedure. A sampling core (Ø 5 cm) was inserted 10 cm deep, filled with filtered sea water and closed with a gas impermeable rubber stopper. A metal core (Ø 9 cm) was inserted around the sampling core to prevent disturbance of the plot and remained in place during the experiment. The sampling core was transported in a dark cool container to the laboratory. The ^{13}C-DIC flux was estimated from the difference in ^{13}C-DIC in the overlying water in the field and the laboratory. Sediment was sliced into three depth intervals (0-2, 2-5 and 5-10 cm), homogenized and sampled for POC, ^{13}C-POC, PLFAs and ^{13}C-PLFAs (5-10 ml wet sediment), porewater DIC and ^{13}C-DIC (15-20 ml wet sediment), meiobenthic biomass and label incorporation (10 ml wet sediment). The remaining sediment ($\sim$ 15 ml for 0-2 cm, $\sim$ 35 ml for 2-5 cm and $\sim$ 75 ml for 5-10 cm) was used to measure label incorporation by macrobenthos. Meiobenthic and macrobenthic samples were fixed with formalin (final concentration 4 %). In this paper we will present total uptake by meiobenthos and macrobenthos, while uptake rates of meiobenthic taxa and macrobenthic species will be presented in a paper that focusses on the importance of bacteria in individual diets (Chapter 5).

4.2.2 Analytical procedures

Sediment samples were weighed, freeze-dried, weighed again and converted to porosity assuming a dry sediment density of 2.55 g cm^{-3}. Organic carbon content and stable isotope ratios of sediment POC, meiobenthos and macrobenthos were measured by elemental analyzer - isotope ratio mass spectrometry (EA-IRMS) (Middelburg et al., 2000). Label incorporation into bacteria was calculated from incorporation in specific bacterial PLFA biomarkers (i14:0, i15:0, a15:0, i16:0 and 18:1ω7c). Lipids were extracted from 3 g dry sediment using a Bligh and Dyer extraction, from which the PLFA fraction was isolated by sequentially rinsing the lipid extract on a silicic acid column with chloroform, acetone and methanol. The PLFA extract was derivatized to volatile fatty acid methyl esters (FAME) and measured by gas chromatography-isotope ratio mass spectroscopy (GC-IRMS) for PLFA concentration and $\delta^{13}C$-PLFA. Full methodological details can be found in Boschker et al. (1999) and Middelburg et al. (2000). Porewater was extracted by centrifugation (Saager et al., 1990) and transferred to a helium flushed headspace vial,

acidified (0.1 ml H_3PO_4 ml^{-1} porewater) and stored upside down. A 3 ml headspace was created in the DIC/^{13}C-DIC bottom water samples by replacing water with He and acidified as described above. DIC and ^{13}C-DIC were determined by EA-IRMS (Moodley et al., 2000).

Meiobenthic samples were sieved (38 μm) and sub-sampled. Specimens of each meiobenthic group were handpicked, typically 15-30 per group, for stable isotope measurements, cleaned of adhering detritus, rinsed (0.2 μm filtered water), transferred to silver boats and stored frozen. Prior to isotope analysis the samples were thawed, acidified for carbonate removal with 20 μl 2.5 % HCl, oven-dried (50 °C) and pinched closed. Meiobenthic biomass was estimated as in Moodley et al. (2002): the carbon content of individual specimens of each meiobenthic group was determined from the carbon signal from the EA-IRMS (calibrated with Cs_2CO_3 standards) and multiplied by the number of organisms in the whole sample. Processing the meiobenthic samples proved to be very time consuming and some sacrifices were made: stable isotope data are based on samples from one plot only and the biomass is estimated from the samples taken at day 0, 0.2, 2, 4 and 6.

All macrobenthos specimens were handpicked from the sample and stored in filtered water and preserved with formalin. The sorted sample was transferred to a petri dish, from which a species sample was taken, rinsed, transferred to a silver boat and stored frozen. Bivalves were placed in an acidified bath (1 mmol HCl) to dissolve the carbonate shell, cleaned of debris, rinsed thoroughly and either whole specimens (small specimens) or flesh samples (large specimens) were transferred to silver boats and stored frozen. Sample treatment prior to isotope analysis was similar to that for meiobenthos. Macrobenthos biomass could not be accurately determined from the small sampling cores and was therefore determined by a dedicated sampling on 27th of May 2003: 12 cores (Ø 10 cm) were taken close to the experimental plots, sliced into 0-2, 2-5, 5-10, 10-20 and $>$ 20 cm intervals, fixed with formalin (4 % final concentration), sieved (1 mm), sorted, weighed for wet weight and finally converted to C units using species specific conversion factors available from a large database at the Netherlands Institute of Ecology.

Delta values are expressed relative to the carbon isotope ratio (R: ^{13}C/^{12}C) of Vienna Pee Dee Belemnite (VPDB): δ^{13}C = (R_{sample}/R_{VPDB} - 1) x 1000, R_{VPDB} is 0.0112372. Label incorporation is presented as total label content in mmol ^{13}C m^{-2} in the top 10 cm (I), where I is calculated as (F_{sample} - $F_{background}$) x S, where F is the ^{13}C fraction (^{13}C /(^{13}C + ^{12}C) = R/(R+1)) and S is the total carbon stock (mmol C m^{-2}) of the respective compartment.

All C and ^{13}C data reported are integrated over the top 10 cm of the sediment and are the mean of the two plots, except for meiobenthos. Errors are reported as standard deviation.

4.2.3 Model description

A mechanistic model was used to simulate the transfer of label among the biotic and abiotic compartments. The model structure was inspired by the bacterial mass balance description of Boudreau (1999), but was assumed to be zero-dimensional as the incorporated processes did not require more complexity. Particulate organic carbon (POC), dissolved organic carbon (DOC) and bacterial carbon dynamics are implemented as C and excess ^{13}C balances, whereas meiobenthos and macrobenthos are modeled only as excess ^{13}C under the assumption that their total biomass is at steady-state (Fig. 4.1). All model variables are listed in Table 4.1, model parameters are in Table 4.2, parameter values are in 4.4 and

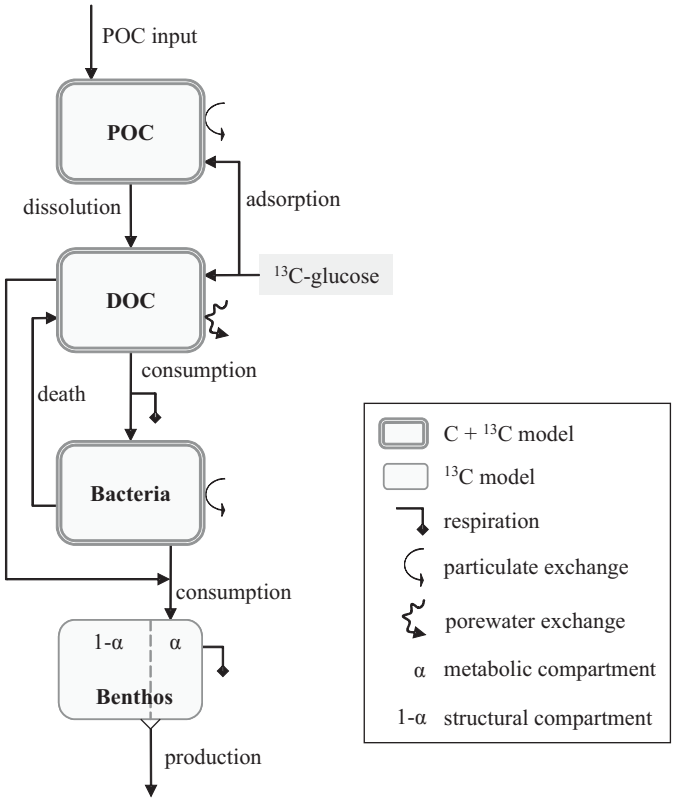

Figure 4.1: Schematic of the model showing the pathways among particulate organic carbon (POC), dissolved organic carbon (DOC), bacteria and benthos. Meiobenthos and macrobenthos are modeled separately but pictured together as benthos for simplicity.

model equations of state variables (s#) and variables (v#) are in Table 4.3.

Table 4.1: Model state variables, variables and forcing functions. The symbol X has a variable interpretation which is detailed in the description.

State variables	**Unit**	**Description**
P	mmol C m^{-2}	particulate organic carbon (POC)
D	mmol C m^{-2}	dissolved organic carbon (DOC)
B	mmol C m^{-2}	bacterial biomass
P_{13C}	mmol ^{13}C m^{-2}	excess ^{13}C in POC
D_{13C}	mmol ^{13}C m^{-2}	excess ^{13}C in DOC
B_{13C}	mmol ^{13}C m^{-2}	excess ^{13}C in bacterial biomass
MxE_{13C}	mmol ^{13}C m^{-2}	excess ^{13}C in metabolic fraction of meio- or macrobenthos
MxS_{13C}	mmol ^{13}C m^{-2}	excess ^{13}C in structural fraction of mass of meio- or macrobenthos
DIC_{13C}	mmol ^{13}C m^{-2}	Accumulated respired excess ^{13}C
Variables	**Unit**	**Description**
F_x	^{13}C/C	fraction ^{13}C of total C

		in compartment x
$f(T)$	-	temperature effect
Me_{13C}	mmol ^{13}C m^{-2}	excess ^{13}C in meiobenthos
Ma_{13C}	mmol ^{13}C m^{-2}	excess ^{13}C in macrobenthos
Org	mmol C m^{-2}	sum of P, D, B, Me, and Ma
Org_{13C}	mmol ^{13}C m^{-2}	sum of P_{13C}, D_{13C}, B_{13C}, Me_{13C}, and Ma_{13C}
$disP_{P,D}$	mmol C m^{-2} d^{-1}	dissolution of POC
$adsGlu_{Glu,P}$	mmol ^{13}C m^{-2} d^{-1}	injected glucose adsorbed to POC
$disGlu_{Glu,D}$	mmol ^{13}C m^{-2} d^{-1}	injected glucose dissolved as DOC
$uptD_{D,B}$	mmol C m^{-2} d^{-1}	uptake of DOC by bacteria
$morB_{B,D}$	mmol C m^{-2} d^{-1}	bacterial mortality
$graM_{B,M}$	mmol C m^{-2} d^{-1}	bacterial grazing by meio- and macrobenthos
$sorM_{D,M}$	mmol C m^{-2} d^{-1}	DOC uptake by meio- and macrobenthos
$proMx$	mmol C m^{-2} d^{-1}	production by meio- (Me) or macrobenthos (Ma)
$excX$	mmol ^{13}C m^{-2} d^{-1}	exchanges of ^{13}C-POC, ^{13}C-DOC or ^{13}C-bacteria

Forcings	**Unit**	**Description**
$Temp$	°C	temperature
$GluInj$	mmol ^{13}C m^{-2} d^{-1}	flux of injected ^{13}C labeled glucose
$POCinput$	mmol C m^{-2} d^{-1}	POC input

The biological processes are influenced by temperature using the Q_{10} formulation (v1). Carbon input to POC is constant (v2), but ^{13}C-glucose injection occurs in a period of 2 hours (v4). POC dissolution (v5) and uptake of DOC by bacteria (v8) are first order processes, which is conceptually equivalent to the common formulation in diagenetic models (Boudreau, 1999). Adsorption of a part of the injected glucose (v3) occurs immediately after amendment (Henrichs and Sugai, 1993). A fixed fraction of the DOC uptake by bacteria is respired and the remainder is incorporated into bacterial biomass (s3, s9). Bacterial mortality is a first order process (v6) and the bacterially derived organic carbon flows to DOC (s2). Exchange processes are a dilution term acting on ^{13}C-POC (e.g., advection, resuspension), ^{13}C-DOC (e.g., diffusion, bioirrigation) and ^{13}C-bacteria (e.g., advection, resuspension) (v11), under the assumption that exchanged labeled carbon is replaced by unlabeled carbon. Most organic matter and bacteria are attached to sediment grains, therefore the exchange rate for POC and bacteria is taken as equal (v11). Meiobenthic and macrobenthic biomass are assumed to be in steady-state. Their biomass, PB ratio and growth efficiency generate a carbon demand (v12), which is fulfilled partly by DOC (v9) and bacteria (v10). The steady-state assumption implies that secondary production by meiobenthos and macrobenthos is balanced by loss processes such as mortality or grazing by higher trophic levels (e.g., fish and birds). In the model, meiobenthos and macrobenthos consist of two compartments: a metabolic and a structural compartment. All assimilated carbon enters the metabolic compartment, turnover of this compartment is due to respiration and production (s7). A continuous flow feeds the structural compartment, of which the turnover is solely due to production (s8).

The model was implemented in the modeling environment FEMME (Soetaert

et al., 2002), the environment and model code can be downloaded from http://www.nioo.knaw.nl/ceme/femme. The model was solved with a 4^{th} order Runge-Kutta integration method with a fixed time step of 0.01 d. A spin-up period of 300 days successfully damped the effect of initial conditions.

Table 4.2: Model parameters.

Symbol	Unit	Description
F_{Glu}	mmol ^{13}C m^{-2} d^{-1}	Glucose injection rate
Q_{10}	-	Temperature dependence
ε_{Glu}	-	Injection efficiency
F_{POC}	mmol C m^{-2} d^{-1}	Input of POC
ε_M	-	Growth efficiency benthos
Me	mmol C m^{-2}	Meiobenthic biomass
Ma	mmol C m^{-2}	Macrobenthic biomass
K_{Glu}	-	Glucose adsorption
$d_{P,D}$	d^{-1}	POC dissolution
λ_P	d^{-1}	POC exchange
λ_D	d^{-1}	DOC exchange
$r_{D,B}$	d^{-1}	Bacterial DOC uptake
ε_B	-	Bacterial growth efficiency
m_B	d^{-1}	Mortality rate
α	-	Metabolic part of biomass
PB_{Me}	d^{-1}	Production rate meiobenthos
β_{Me}	-	Bacteria in meiobenthos diet
ρ_{Me}	-	DOC in meiobenthos diet
PB_{Ma}	d^{-1}	Production rate macrobenthos
β_{Ma}	-	Bacteria in macrobenthos diet
ρ_{Ma}	-	DOC in macrobenthos diet

Table 4.3: Model equations. The miscellaneous symbol X is specified for every state variable or variable. The symbol Mx stands for both Me and Ma.

(v1)	$f(T) = Q_{10}^{\frac{Temp-20}{10}}$
(s1)	$\frac{dP}{dt} = POCinput + adsGlu_{Glu,P} - disP_{P,D}$
(v2)	$POCinput = Flux_{POC}$
(v3)	$adsGlu_{Glu,P} = \varepsilon_{Glu} \cdot K_{Glu} \cdot GluInj$
(v4)	$GluInj = Flux_{Glu} \cdot H(t)$ with $H(t) = \begin{cases} 1, & 0 \leq t \leq 0.08, 2 \leq t \leq 2.08, 3 \leq t \leq 3.08, 4 \leq t \leq 4.08 \\ 0, & otherwise \end{cases}$
(v5)	$disP_{P,D} = d_{P,D} \cdot f(T) \cdot P$
(s2)	$\frac{dD}{dt} = disP_{P,D} + morB_{B,D} + disGlu_{Glu,D} - uptD_{D,B} - sorM_{D,M}$
(v6)	$morB_{B,D} = m_B \cdot f(T) \cdot B$
(v7)	$disGlu_{Glu,D} = \varepsilon_{Glu} \cdot (1 - K_{Glu}) \cdot GluInj$
(v8)	$uptD_{D,B} = r_{D,B} \cdot f(T) \cdot D$
(v9)	$sorM_{D,M} = f(T) \cdot {\varepsilon_M}^{-1} \cdot (\rho_{Me} \cdot PB_{Me} \cdot Me + \rho_{Ma} \cdot PB_{Ma} \cdot Ma)$
(s3)	$\frac{dB}{dt} = \varepsilon_B \cdot uptD_{D,B} - morB_{B,D} - graM_{B,M}$

(v10) $graM_{B,M} = f(T) \cdot {\varepsilon_M}^{-1} \cdot (\beta_{Me} \cdot PB_{Me} \cdot Me + \beta_{Ma} \cdot PB_{Ma} \cdot Ma)$

(s4) $\frac{dP_{13C}}{dt} = adsGlu_{Glu,P} - (disP_{P,D} + excP) \cdot F_P$

(v11) $excX = \lambda_X \cdot X$ with λ_X for λ_P and λ_D, and X for P, D, and B

(s5) $\frac{dD_{13C}}{dt} = disGlu_{Glu,D} + disP_{P,D} \cdot F_P + morB_{B,D} \cdot F_B$
$-(uptD_{D,B} + sorM_{D,M} + excD) \cdot F_D$

(s6) $\frac{dB_{13C}}{dt} = \varepsilon_B \cdot uptD_{D,B} \cdot F_D - (morB_{B,D} + graM_{B,M} + excB) \cdot F_B$

(s7) $\frac{dMxE_{13C}}{dt} = graMx_{B,Mx} \cdot F_B + sorMx_{D,Mx} \cdot F_D - {\varepsilon_M}^{-1} \cdot proMx \cdot F_{MxE}$

(v12) $proMx = f(T) \cdot PB_{Mx} \cdot Mx$

(s8) $\frac{dMxS_{13C}}{dt} = (1 - \alpha) \cdot proMx \cdot (F_{MxE} - F_{MxS})$

(v13) $Mx_{13C} = MxE_{13C} + MxS_{13C}$

(s9) $\frac{dDIC_{13C}}{dt} = (1 - \varepsilon_B) \cdot uptD_{D,B} \cdot F_D + \left(\frac{1-\varepsilon_M}{\varepsilon_M}\right) \cdot proMx \cdot F_{MxE}$

(v14) $Org = P + D + B + Me + Ma$

(v15) $Org_{13C} = P_{13C} + D_{13C} + B_{13C} + Me_{13C} + Ma_{13C}$

4.2.4 Calibration and uncertainty analysis

Initial ranges of parameter values were taken from the literature (Table 4.4). The optimal parameter set was subsequently selected from these ranges by minimization of a weighted cost function

$$J = \sum_{i=1}^{NVar} \sum_{j=1}^{NObs} \frac{(M_{ij} - O_{ij})^2}{\sigma_i} \tag{4.1}$$

in which all ($NObs$) model (M_{ij}) versus observation (O_{ij}) deviations are squared and weighed by the standard deviation σ_i for all variables ($NVar$). The σ_i is the average standard deviation for each variable. The parameter set which had the lowest cost function produces the best fit to the data.

Pools of bacterial carbon and POC show significant variation over the season and when the model is fitted to these data, this variation dominates the cost function. The first order model described here is suitable to track exponential-like tracer kinetics, but is inappropriate to model short-term temporal and spatial variation. To alleviate the impact of varying bacterial and POC pools on the cost function, the season-averaged pool size and standard deviation have been evaluated in the cost function instead of the original data (see also 4.4 Discussion). This ensures a correct order of magnitude pool size, but moderates the impact on the cost function. A pseudo-random calibration method (25000 runs and population size 500) was chosen because of its ability to locate the global minimum in a large parameter space (Price, 1979). The calibration ended with 250 runs of the Levenberg-Marquardt gradient method (Press et al., 1992), because of its ability to quickly converge to the minimum, once in a valley.

Parameter uncertainty, induced by fitting a model to uncertain data, was estimated by Bayesian inference (Gelman et al., 2003), using a Markov Chain Monte Carlo technique (Gilks et al., 1998). The Markov chain was initiated with the best-fit solution resulting from the calibration; it was terminated when 2000 draws were selected. The mean and standard deviation of the model parameters were then calculated from the selected draws.

Table 4.4: The initial ranges of the model parameters taken from the literature sources 1) Widdows et al. (2004), 2) review in Van Oevelen et al. (Chapter 3), 3) Henrichs and Sugai (1993), 4) Westrich and Berner (1984), 5) Henrichs and Doyle (1986), 6) Dauwe et al. (2001), 7) Widdows et al. (2000), 8) Martin and Banta (1992), 9) Schluter et al. (2000), 10) Meile et al. (2001), 11) Arnosti and Holmer (1999), 12) del Giorgio and Cole (1998), 13) Anderson and Williams (1999), 14) Fischer et al. (2003), 15) Mei and Danovaro (2004) and 16) Van Oevelen et al. (Chapter 5). Bayesian analysis (see 4.2 Material and methods) produces a set of accepted parameter values, which are presented as mean $\pm$ standard deviation. Parameters with no initial range were fixed in the simulations.

Symbol	Initial range	Value	Source
F_{Glu}		183	
Q_{10}		2	
ε_{Glu}		0.74	[a]
F_{POC}		52	1
ε_M		0.50	2
Me		188	sampled
Ma		1624	sampled
K_{Glu}	0.29-0.39	0.34$\pm$0.025	3
$d_{P,D}$	0.0005-0.003	0.0024$\pm$0.00024	4,5,6
λ_P	0.0-0.093	0.0085$\pm$0.0024	7
λ_D	0.05-1.00	0.58$\pm$0.14	8,9,10
$r_{D,B}$	0.08-2.67	0.46$\pm$0.12	11
ε_B	0.40-0.75	0.50$\pm$0.03	12
m_B	0.0-0.14	0.07$\pm$0.02	13,14,15
α	0.0-0.50	0.31$\pm$0.11	assumed
PB_{Me}	0.03-0.09	0.065$\pm$0.014	2
β_{Me}	0.05-0.15	0.097$\pm$0.024	16
ρ_{Me}	0.0-0.15	0.036$\pm$0.012	assumed
PB_{Ma}	0.01-0.05	0.028$\pm$0.009	2
β_{Ma}	0.08-0.30	0.20$\pm$0.05	16
ρ_{Ma}	0.0-0.15	0.094$\pm$0.032	assumed

[a] defined as the amount of label recoverable after the first 4 hours

4.3 Results

4.3.1 Organic carbon pools

Sediment POC content averaged 0.48 % wt/wt and porosity was 0.50, corresponding to a POC pool of 46.6 mol C m^{-2} in the upper 10 cm of the sediment. The benthic community was dominated by macrobenthos (1624 mmol C m^{-2}), followed by bacteria (781 mmol C m^{-2}) and meiobenthos (188 mmol C m^{-2}) (Table 4.5). Meiobenthic biomass was dominated by nematodes and foraminifera. Macrobenthic was dominated by large specimens of the bivalve *Macoma balthica* and the polychaetes, *Heteromastus filiformis* and *Pygospio elegans*.

Table 4.5: Biomass of bacteria, meiobenthos and macrobenthos (mmol C m^{-2}).

Compartment	**Biomass**
Bacteria	781
Meiobenthos	188
Nematodes	67
Hard-shelled foraminifera	62
Juveniles *Heteromastus filiformis*	34
Unknown	9
Soft-bodied foraminifera	6
Turbellaria	4
Polychaetes	4
Copepods	3
Macrobenthos	1624
Macoma balthica ($>$ 7 mm)	671
Heteromastus filiformis	597
Pygospio elegans	215
Polydora cornuta	34
Macoma balthica ($\leq$ 7 mm)	28
Hydrobia ulvae	24
Nereis (Hediste) spp.	21
Eteone sp.	16
Corophium spp.	16
Streblospio benedicti	1

4.3.2 Labeling trajectories and model fits

Excess ^{13}C in the total organic carbon pool, comprising excess ^{13}C in DOC, POC and benthos, increased steadily during the labeling period (except for the dip at day 2 caused by the canceled injection) and peaked at 26.5 mmol ^{13}C m^{-2} on day 5 at the end of the labeling period (Fig. 4.2A). At day 5, about 50 % of the total injected 61.1 mmol ^{13}C m^{-2} was recovered as excess organic (44 %) and respired (8 %) carbon. The initial ^{13}C-POC decrease was high, but slowed after day 20, reflecting turnover differences of the organic carbon pools. After 4.5 months, almost no excess ^{13}C was detected in the organic carbon pool. Bacterial label incorporation was linear over the first 8 days and reached a maximum of 5.1 mmol ^{13}C m^{-2} corresponding to 0.62 mmol ^{13}C m^{-2} d^{-1}, after which it decreased in an exponential fashion (Fig. 4.2B). Meiobenthic label incorporation was swift and peaked around day 10 at 0.07 mmol ^{13}C m^{-2} (Fig. 4.2C), representing 0.02 % of the label in the organic carbon pool. The excess ^{13}C in meiobenthos decreased exponentially and returned to background levels at the end of the experiment. Macrobenthic labeling was rapid within the first 10 days and reached 0.78 mmol ^{13}C m^{-2} at day 5. The labeling variability was mainly caused by variable labeling of the biomass dominating large *M. balthica* (species data not shown). Label decreased exponentially with time and after 4.5 months, 0.1 mmol ^{13}C m^{-2} resided in macrobenthos (Fig. 4.2D). The injected ^{13}C-glucose was rapidly respired to ^{13}C-DIC, as evidenced by the 0.46 mmol ^{13}C m^{-2} respiration in the first 6 hours of the experiment (Fig. 4.2E). The respiration rate of ^{13}C label was highest during the injection period, in which 4.7 mmol ^{13}C m^{-2} was respired. The respiration rate slowed down after the ^{13}C-glucose injection and decreased further after day 36, when a

total of 7 mmol ^{13}C m^{-2} had been respired. In the whole experimental period a total of 8.9 mmol ^{13}C m^{-2} was respired, which corresponds to 15 % of the total ^{13}C addition.

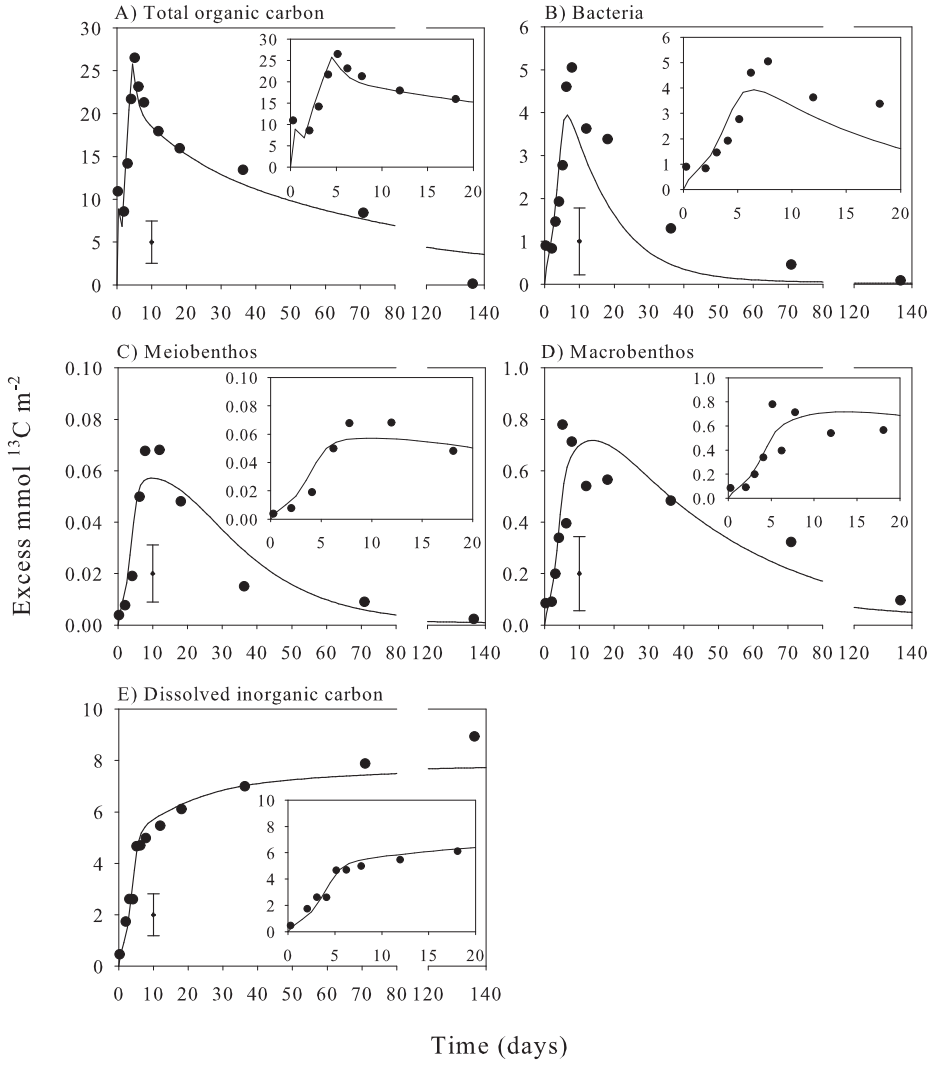

Figure 4.2: Excess ^{13}C in the compartments total organic carbon, bacteria, meiobenthos, macrobenthos and dissolved inorganic carbon with model-derived lines. Plotted data are averages from the two plots and error bars in the plot are the average standard deviations used in the calibration routine (see 4.2 Material and methods). Note the scale break in the time axis. The insets detail the temporal evolution in the first 20 days.

The ^{13}C dynamics of the organic carbon pool were accurately reproduced by the model in the first two months, but excess ^{13}C is overestimated by the model at day 136 (Fig. 4.2A). Modeled bacterial label incorporation tracks the observations during the first 6 days of the experiment, but the observations show a continued incorporation until day 8, which is not well reproduced by the model (Fig. 4.2B). This initial underestimation of label incorporation has repercussions for the prediction during the remainder of the

experiment. The rate at which label disappears from the bacterial compartment also seems higher than observed in the field. Bacterial secondary production averaged 66.5 mmol C m^{-2} d^{-1} and bacterial growth efficiency (BGE) was estimated at 0.50±0.03 (Table 4.4). The label trajectories of meiobenthos and macrobenthos are accurately described, as the magnitude of labeling and their dynamics correspond well to the field observations (Fig. 4.2C and 4.2D). Secondary production by meiobenthos and macrobenthos averaged 11.5 mmol C m^{-2} d^{-1} and 42.5 mmol C m^{-2} d^{-1}, respectively. Respiration of ^{13}C label is very well described during the first 3 months, but the model underestimates the respiration slightly thereafter (Fig. 4.2E). Overall, a plot of model predictions versus field observations reveals a highly significant linear relation that covers data over 4 orders of magnitude, with a slope not significantly different from 1 (Fig. 4.3).

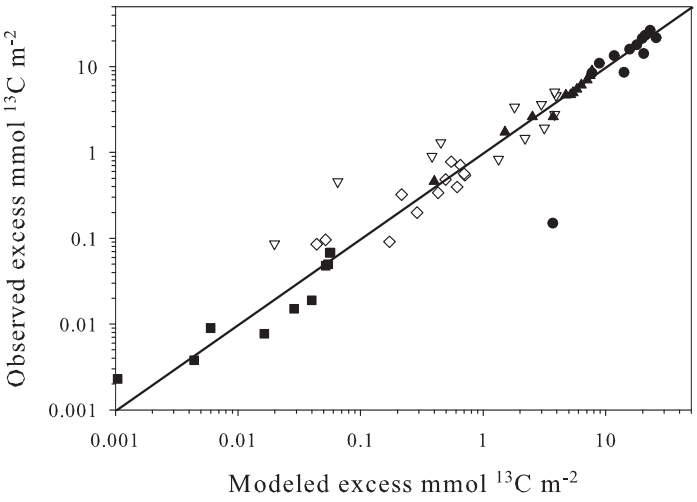

Figure 4.3: Observed versus modeled values of excess mmol ^{13}C m^{-2} in the various model compartments. The line represents the linear regression of all data points ($y = 0.97x, r^2 = 0.95, p < 0.0001, n = 58$).

Some model parameters are more constrained by the observations than others (Table 4.4). The standard deviation relative to the mean is $\leq$ 10 % for the parameters bacterial growth efficiency (ε_B), glucose adsorption (K_{Glu}) and POC dissolution rate ($d_{P,D}$) and between 24 - 37 % for the other parameters, which is similar to the relative error of the observations. Although many parameters have a high relative standard deviation, they are well constrained with regard to their initial range. The parameters POC dissolution rate ($d_{P,D}$), POC exchange rate (λ_P), bacterial DOC uptake rate ($r_{D,B}$), bacterial mortality (m_B), fraction DOC in meiobenthic diet (ρ_{Me}) and macrobenthos production rate (PB_{Ma}) are well constrained as compared to their initial range. However, for the parameters α (metabolic fraction of benthos), β_{Me} (bacterial fraction in meiobenthic diet), PB_{Me} (production rate meiobenthos), ρ_{Ma} (DOC fraction in macrobenthos diet) and K_{Glu} (glucose adsorption constant) the standard deviation is still high as compared to the initial range and these parameters are less constrained by the observations.

4.4 Discussion

This is the first in situ study on the short and long-term fate of benthic bacterial carbon production (BP). Tracking BP was achieved by injecting ^{13}C-glucose into the sediment as a stable isotope tracer and subsequently following this tracer in bacteria, meiobenthos, macrobenthos, total organic carbon and inorganic carbon. Labeling was conducted on several consecutive days to follow uptake kinetics and to ensure sufficient labeling of the bacteria. Subsequently, label appearance and retention was monitored over a period of 4.5 months to provide information on transfer among and turnover of the different compartments. We interpret this extensive data set by means of a mechanistic model that resolves most bacterial gain and loss processes. A mechanistic model requires an explicit description of its structure, underlying assumptions and contains interpretable parameters. Simpler models can be used, but these only use a subset of the available data. For example, label disappearance can be fitted with an exponential decay model to obtain the compartments turnover rate. In this simpler analysis however, data on uptake kinetics are ignored, rate constants represent net turnover as uptake of label continues after label injection, and the model fit is not constrained by any of the other observations. Moreover, the use of a mechanistic model allows us to derive information on unmeasured processes. For instance, bacterial mortality was not measured explicitly, but was derived from the model.

Inherent in benthic microbial ecology are methodological shortcomings and our experimental approach is no exception. These are partly caused by our intention to conduct this experiment over a long time scale in situ, which precludes core incubations. Label was introduced to the sediment in injection wells at a high resolution, but heterogeneous label distribution is inevitable. However, injection is the preferred method to introduce label, while minimizing sediment disturbance (Dobbs et al., 1989). Label uptake by non-grazing processes has been reported by Carman (1990) and therefore poisoned controls have been recommended to distinguish among the uptake pathways (Montagna, 1995), but such controls are not possible on the scale of this experiment. However, turnover time of glucose ($\sim$ hours) is much shorter than that of bacteria ($\sim$ weeks), which allows to distinguish direct uptake of glucose from bacterial grazing at the time scale of the experiment. Another concern was the potential use of respired ^{13}C by microphytobenthos. Fixation of ^{13}C-DIC enriches microphytobenthos into an alternative ^{13}C resource, thus complicating the interpretation of carbon transfer from bacteria to meiobenthos and macrobenthos. Microphytobenthos labeling was assessed through the PLFA biomarkers C20:5ω3 (Middelburg et al., 2000), which increased in δ^{13}C from -22.8 to 19.8 ‰ (day 8) and remained above 5.0 ‰ till day 23. This labeling is lower than the δ^{13}C of most grazers (Van Oevelen et al., (Chapter 5)) and much lower than the δ^{13}C of bacterial biomarkers (between 100 - 500 ‰ during the first month). Hence, recycling of ^{13}C via microphytobenthos does not seriously complicate the interpretation. Finally, glucose addition was truly at tracer level, as the rate of label incorporation (0.62 mmol ^{13}C m^{-2} d^{-1}) represented 0.9 % of total bacterial production (66.5 mmol C m^{-2} d^{-1}).

4.4.1 Model complexity and performance

Model complexity was a compromise between biological realism and data availability. The 0-D representation was one way to minimize model complexity. Among the depth intervals there were minor and quasi-random differences in bacterial and organic carbon δ^{13}C. Therefore, the information gain in a 1-D representation would not outweigh the

necessary additional model parameters. Moreover, a 1-D model description in terms of biomass, feeding and mixing of meiobenthos and macrobenthos is not straightforward.

Sediment organic carbon is characterized by large differences in reactivity (Westrich and Berner, 1984; Middelburg, 1989). Two pools with different lability were distinguished: labile DOC and less reactive POC. This distinction is required as glucose is very labile compared to bulk sediment organic carbon. The fitted rate constant for the DOC pool (0.46 d^{-1}, Table 4.4) is somewhere between the high rate constant of injected glucose and lower rate of DOC that is derived from bacteria or POC. However, data on ^{13}C were only available for total organic carbon and more complexity than two organic carbon pools could therefore not be justified.

Bacterial biomass varied considerably and was generally between 500 - 1300 mmol C m^{-2}. The bacterial biomass in the model was fitted to a constant overall average (781 mmol C m^{-2}) and the model output therefore showed little variation (600 - 800 mmol C m^{-2}). There were several reasons for this approach. There was hourly/daily variation and a more seasonal-like trend on the scale of weeks/months. Short-term variation of a factor 2-3 is inherent in many bacterial biomass estimates and likely contains an important spatial component. This variation cannot be reproduced using the first-order 0-D model that is designed to reproduce excess ^{13}C patterns. The long-term variation shows a general increase in biomass during the first 2-3 weeks of the experiment and then a decrease. Temperature dependence alone cannot explain the biomass evolution because temperature increased during the initial 3 months. We ran simulations with higher bacterial carbon (1000 mmol C m^{-2}) than the season-average, which clearly improved the fit of excess ^{13}C in bacteria, but did not change the general conclusions as presented here. Therefore it is likely that the model fit of the excess bacterial ^{13}C would improve, if the bacterial biomass evolution were better reproduced.

The faunal biomass was modeled as two compartments: a metabolic and a structural compartment (s7 and s8 in Table 4.3). Turnover is faster in the metabolic pool as this pool fuels respiration. This formulation was chosen for its higher realism (Conover, 1961), success in earlier applications (Lehman et al., 2001; Pace et al., 2004), better resemblance to the dynamic energy budget theory (Kooijman, 2000) and improved capability of reproducing the observations.

Finally, it should be stressed that different data weighting schemes and model scenarios were thoroughly tested to assess the robustness of the model results. Model scenarios with no DOC sorption by the benthos typically show a lag in labeling, delayed peak labeling and higher loss rate as compared to the observations. In general, the model results are robust and accurately describe the general trends in the labeling patterns.

4.4.2 Bacterial growth efficiency and production

The bacterial dominance of benthic secondary production has been reported earlier (e.g. Schwinghamer et al. (1986)) and is confirmed in this study with bacteria accounting for 55 % of the secondary production. The parameter BGE was calibrated at 0.50, but as the calibration is based on the respiration of relatively labile compounds (^{13}C-glucose and bacterially derived DOC), the derived BGE is likely an overestimate of the overall BGE.

The regression models presented by Sander and Kalff (1993) predict bacterial production (66.5 mmol C m^{-2} d^{-1}) reasonably when based on bacterial carbon (91 mmol C m^{-2} d^{-1}) or POC (42 mmol C m^{-2} d^{-1}), but their temperature model (15 mmol C m^{-2} d^{-1}) underestimates our bacterial production.

Boudreau (1999) presented detailed mass balances of bacterial carbon in sediments

and scaled the mass balance terms to arrive at a linear relation between bacteria and POC. The parameters of this linear relation are composed of parameters for irrigation, advection, bacterial production, mortality, grazing and bacterial growth efficiency. When the parameters obtained in our study are implemented in Boudreau's scaled linear model, the predicted ratio between bacterial biomass and POC is 0.005, consistent with, but at the lower end of the observed ratios, ranging from 0.005 to 0.024. The predicted bacterial biomass to POC ratio is based on interpretative and measurable parameters, rather than regression parameters. The general agreement is certainly encouraging, but additional data sets are required to test the general predictive power.

4.4.3 Label pathways

The use of a mechanistic model not only allow to reproduce the observations and derive useful model parameters, but also provided detailed information on the relative contributions of the different ^{13}C pathways (Fig. 4.4). The importance of the ^{13}C loss pathways from the sediment changed considerably with time. Initially, label loss occurs mainly through exchange of DOC (75 %) and respiration (20 %) but after a few days POC resuspension dominates (Fig. 4.4A). Meiobenthos and macrobenthos turnover account for maximal 10 % of the label loss. The importance of the pathways differed with time, indicating that extrapolation from short-term experiments should be done with caution. The fate of bacterial carbon production was rather invariant during the experiment and was partitioned among resuspension (8 %), meiobenthos grazing (3 %), macrobenthos grazing (24 %) and mortality (65 %) (Fig. 4.4B). The label sources for macrobenthos (very similar for meiobenthos) reflect the different turnover rates of DOC and bacteria. During the first 5 day period of label addition, 75 % of label incorporation was related to sorption of DOC, but within 2 days of ending the label injections bacterivory dominated label incorporation (90 %) and remained high thereafter (Fig. 4.4C).

4.4.4 Fate of bacterial carbon production

The microbial loop has been formalized as bacterial assimilation of dissolved organic matter and subsequent transfer up the food web by bacterivory and predation on bacterivores (Azam et al., 1983). The significance and efficiency of this loop has focussed on a link or sink debate: is bacterial production a carbon link or sink in the food web? The intractable benthic environment has made experimental studies difficult and studies therefore have tended to focus on a subset of potential grazers, such as heterotrophic flagellates (Hondeveld et al., 1995; Hamels et al., 2001b), meiobenthos (Montagna, 1995) or macrobenthos species (Kemp, 1987; Grossmann and Reichardt, 1991). These studies dealing with a subset of the grazers revealed that 1 - 20 % of the bacterial production is grazed. For the present study site, bacterial grazing by the total benthic community in the top 10 cm of the sediment was quantified. We estimate that $\sim$ 30 % of the bacterial production was grazed: 1 - 2 % by microbenthos (1.1 mmol C m^{-2} d^{-1} from Hamels et al. (1998)), 3 % by meiobenthos (this study) and 24 % by macrobenthos (this study). As meiobenthos and macrobenthos biomass at our study sites are high as compared to other sediments (Heip et al., 1995), we assert that bacterivory is comparatively intense. Given the accumulated evidence, grazing can be regarded as a minor to moderate fate of bacterial production in sediments.

Our combined experimental and modeling approach allowed us to distinguish among the bacterial loss pathways grazing, resuspension and mortality. Bacterial mortality

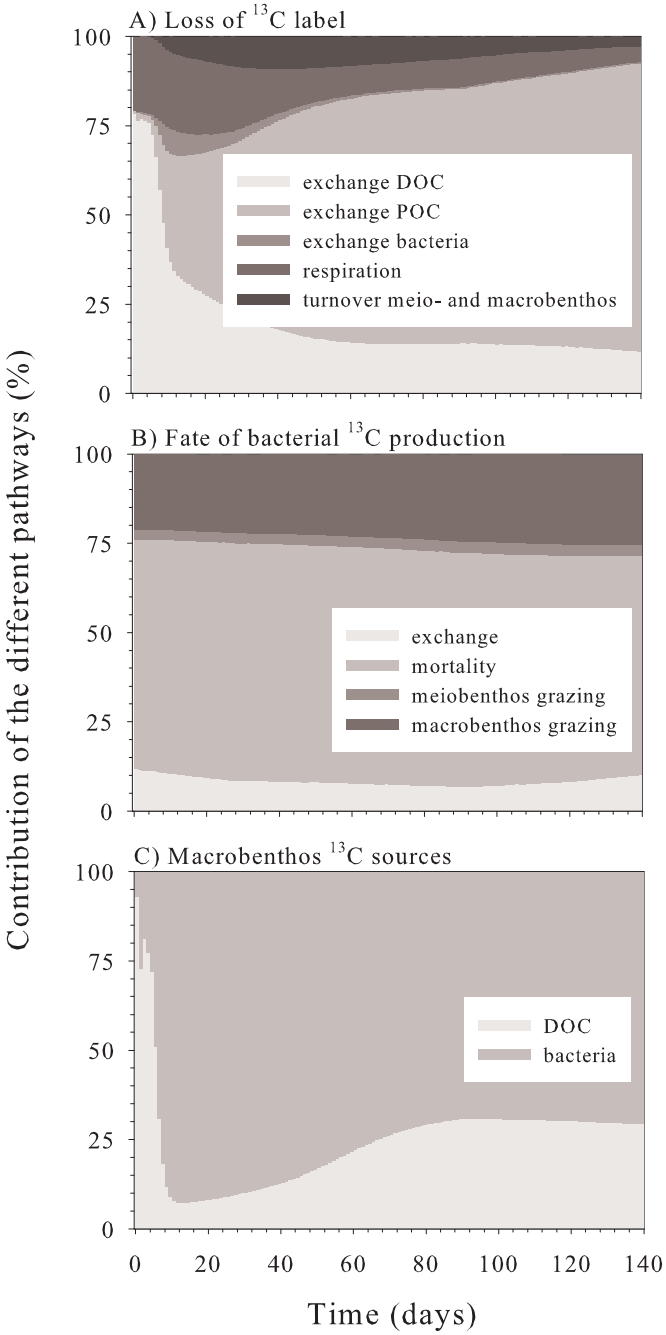

Figure 4.4: Percentage contribution of excess ^{13}C pathways in the A) loss of ^{13}C from the sediment, B) fate of bacterial ^{13}C production and C) macrobenthos ^{13}C sources.

appeared to dominate and represented a sink of 65 % of the bacterial production. However, the cause of bacterial mortality remains unexplained. Several mortality causes are known. Bacterial cell lysis resulting from a lytic infection by viruses is a major cause of bacterial

mortality in pelagic systems (Weinbauer, 2004), and was thought to be similarly important in sediments, because of higher viral and bacterial abundances (Paul et al., 1993; Maranger and Bird, 1996; Mei and Danovaro, 2004). Recent estimates on the contribution of viral lysis to bacterial mortality show a large range of 0 - 40 % (Ricciardi-Rigault et al., 2000; Hewson and Fuhrman, 2003; Glud and Middelboe, 2004). Therefore, viral lysis may be an important cause of bacterial mortality but large differences in reported contributions do not warrant generalization of the importance of this process. Programmed cell death, mortality caused by triggering an intracellular genetic code, has been found in bacterial cultures (Yarmolinsky, 1995; Engelberg-Kulka and Glaser, 1999), but remains to be quantified for natural bacterial populations. Similarly, environmental factors such as the presence of toxic compounds and thermal or salinity stress may cause mortality, but their quantitative importance remains unknown. Several factors causing bacterial mortality, other than grazing, are not yet or only recently being explored and their importance remains to be established. Irrespective of the cause of death, non-grazing mortality results in the release of bacterially derived carbon that is potentially available for recycling back to DOC.

Recycling in the DOC - bacteria loop was evaluated by a recycling efficiency, defined as $E = \frac{Bacterial\ death}{Bacterial\ DOC\ uptake}$ and the average number of cycles in the loop of a carbon molecule as $R = \frac{Bacterial\ death}{POC\ dissolution + DOC\ exchange}$, both based on season-averaged flow values. The recycling efficiency may vary between 0 (no recycling) and 1 (full recycling) and R between 0 (molecule cycles zero times) and ∞ (molecule cycles infinitely). The recycling efficiency for the DOC - bacterial loop was moderate (0.36). Note that respiration losses cap E to a maximum of 0.50 (i.e. ε_B = 0.50, Table 4.4), which implies that 72 % (i.e. 0.36/0.50) of the bacterial production is recycled back to the DOC pool. Despite moderate recycling, R was comparatively low (0.17) due to the high exchange rate of DOC that dominates over the flux from bacteria to DOC. Recycling of bacterially derived carbon is consistent with observations that bacterial lysate is readily degraded by natural communities (Novitsky, 1986; Middelboe et al., 2003). However, several studies document the accumulation of the bacterial cell wall derived D-Alanine in oceans (McCarthy et al., 1998) and continental margin sediments (Grutters et al., 2002). In a companion paper (Veuger et al. (Chapter 6)), the ^{13}C in D-Alanine is compared with that in labile PLFAs and the results suggest that burial of bacterial remnants is not a major sink for bacterial carbon, but instead is recycled back to the DOC pool.

Alongi (1994) speculated on the role of bacterial cycling in tropical benthic systems and asserted that the majority of bacterial production remains ungrazed but instead lyses and the lysate is recycled within the bacterial community. Such a bacterial-viral loop was recently also proposed for pelagic food webs (Fuhrman, 2000). Our comprehensive study on the fate of benthic bacterial carbon production agrees with this concept, although the cause of death may not necessarily be viral lysis. The observed recycling is also consistent with the well documented efficient recycling of ammonium in sediments with net rates of regeneration being a fraction of gross ammonification (Blackburn and Henriksen, 1983).

Finally, the advent of diagenetic models that explicitly include bacterial biomass (Talin et al., 2003) requires an appropriate parametrization of benthic bacterial dynamics. The correspondence between the mass balance model developed by Boudreau (1999) and our results suggests a promising avenue for further exploration.